

University of Windsor

Scholarship at UWindor

Electronic Theses and Dissertations

Theses, Dissertations, and Major Papers

2022

A Preliminary Study of Electrode Geometry Impact on Spark Discharge Processes

Hongyang Shangguan
University of Windsor

Follow this and additional works at: <https://scholar.uwindsor.ca/etd>



Part of the [Mechanical Engineering Commons](#)

Recommended Citation

Shangguan, Hongyang, "A Preliminary Study of Electrode Geometry Impact on Spark Discharge Processes" (2022). *Electronic Theses and Dissertations*. 9123.
<https://scholar.uwindsor.ca/etd/9123>

This online database contains the full-text of PhD dissertations and Masters' theses of University of Windsor students from 1954 forward. These documents are made available for personal study and research purposes only, in accordance with the Canadian Copyright Act and the Creative Commons license—CC BY-NC-ND (Attribution, Non-Commercial, No Derivative Works). Under this license, works must always be attributed to the copyright holder (original author), cannot be used for any commercial purposes, and may not be altered. Any other use would require the permission of the copyright holder. Students may inquire about withdrawing their dissertation and/or thesis from this database. For additional inquiries, please contact the repository administrator via email (scholarship@uwindsor.ca) or by telephone at 519-253-3000ext. 3208.

**A Preliminary Study of Electrode Geometry Impact on Spark Discharge
Processes**

By

Hongyang Shangguan

A Thesis
Submitted to the Faculty of Graduate Studies
through the Department of Mechanical, Automotive, and Materials Engineering
in Partial Fulfillment of the Requirements for
the Degree of Master of Applied Science
at the University of Windsor

Windsor, Ontario, Canada

2022

© 2022 Hongyang Shangguan

A Preliminary Study of Electrode Geometry Impact on Spark Discharge Processes

by

Hongyang Shangguan

APPROVED BY:

X. Xu

Department of Civil and Environmental Engineering

J. Tjong

Department of Mechanical, Automotive and Materials Engineering

X. Yu, Co-Advisor

Department of Mechanical, Automotive and Materials Engineering

M. Zheng, Co-Advisor

Department of Mechanical, Automotive and Materials Engineering

September 07, 2022

DECLARATION OF ORIGINALITY

I hereby certify that I am the sole author of this thesis and that no part of this thesis has been published or submitted for publication.

I certify that, to the best of my knowledge, my thesis does not infringe upon anyone's copyright nor violate any proprietary rights and that any ideas, techniques, quotations, or any other material from the work of other people included in my thesis, published or otherwise, are fully acknowledged in accordance with the standard referencing practices. Furthermore, to the extent that I have included copyrighted material that surpasses the bounds of fair dealing within the meaning of the Canada Copyright Act, I certify that I have obtained a written permission from the copyright owner(s) to include such material(s) in my thesis and have included copies of such copyright clearances to my appendix.

I declare that this is a true copy of my thesis, including any final revisions, as approved by my thesis committee and the Graduate Studies Office, and that this thesis has not been submitted for a higher degree to any other University or Institution.

ABSTRACT

The ever-growing demands to meet the exhaust emission regulations and fuel economy requirements have driven the development of modern spark ignition (SI) engines towards lean/diluted combustion strategies and engine downsizing. Currently, the transistor coil ignition (TCI) system is still the dominant ignition system applied in SI engines. This work investigates the effects of electrode diameters on the spark discharge characteristics.

In this study, different electrode diameters (0.2 mm, 0.7 mm, 1.5 mm, and 3.5mm) are used. The electrical waveforms of the discharge process are recorded, including the breakdown voltage, the glow voltage, and the secondary current. Results show that the breakdown voltage increases with the increase of electrode diameters (including high-voltage (HV) and ground electrodes). Besides, the glow voltage decreases with the electrode diameters increase.

DEDICATION

This thesis is dedicated to my family, who have always been supportive of my
life.

ACKNOWLEDGEMENTS

First of all, I would like to express my gratitude to Dr. Ming Zheng, my academic supervisor, who gave me the opportunity to take a part in the Clean Combustion Engine Lab and guided me throughout my master's degree studies at the University of Windsor. I would like to thank my co-advisor, Dr. Xiao Yu, for his advice and guidance throughout my study. Their wisdom and enthusiasm for research have inspired me to face every challenge encountered throughout the development of this thesis.

I would like to acknowledge the thesis committee members, Dr. Jimi Tjong and Dr. Xiaohong Xu for their precious time, giving me constructive criticism and guidance on my thesis.

Thanks to all my dear colleagues at the Clean Combustion Engine Laboratory, Dr. Meiping Wang, Dr. Hua Zhu, Dr. Zhenyi Yang, Linyan Wang, Simon Leblanc, Navjot Sandhu, Long Jin, Alex Bastable, Binghao Cong, and Muyu Guo, your enormous support has been greatly appreciated. I would like to thank Linyan Wang for her invaluable advice and her support with the programming. I would like to thank Linyan Wang and Simon Leblanc for their help with the experiments.

Finally, I would like to thank my parents for their love and support all the time.

TABLE OF CONTENTS

DECLARATION OF ORIGINALITY	iii
ABSTRACT	iv
DEDICATION	v
ACKNOWLEDGEMENTS	vi
LIST OF TABLES	ix
LIST OF FIGURES	x
LIST OF ABBREVIATIONS/SYMBOLS	xii
CHAPTER 1 INTRODUCTION	1
1.1 Background	1
1.2 Ignition System and Spark Discharge Principle.....	1
1.3 Challenges of the Current Ignition Systems.....	5
1.4 Literature Review	6
1.5 Objective of the Thesis.....	8
1.6 Structure of the Thesis.....	8
CHAPTER 2 EXPERIMENTAL SETUP	10
2.1 Overview of the Experimental Setup	10
2.2 Spark Plug	11
2.3 Ignition Coil	12
2.4 Control System.....	13
2.4.1 Signal Splitter	13
2.4.2 Ignition Coil Driver	13
2.5 Measurement and Data Acquisition Devices	14
2.5.1 Measurement Devices.....	14
2.5.2 Data Acquisition Devices	15

CHAPTER 3 THE IMPACT OF ELECTRODES DIAMETERS ON BREAKDOWN VOLTAGE.....	16
3.1 Data Processing and Calculation Method of the Breakdown Voltage	16
3.2 Impact of Electrodes Diameter on the Breakdown Voltage.....	18
CHAPTER 4 THE IMPACT OF ELECTRODE DIAMETER ON GLOW PHASE.....	22
4.1 Impact of Electrodes Diameter on the Glow Voltage	25
4.2 Impact of Electrodes Diameter on the Discharge Energy	26
4.3 Impact of Electrodes Diameter on the Discharge Duration	28
CHAPTER 5 CONCLUSIONS AND FUTURE WORK.....	30
5.1 Conclusions	30
5.2 Future Work	31
REFERENCES	32
VITA AUCTORIS	38

LIST OF TABLES

Table 2.1 Specifications of MSD Ignition 5527 coil	12
Table 2.2 Specifications of the data acquisition devices	14
Table 2.3 Specifications of the PicoScope 4425	15

LIST OF FIGURES

Figure 1.1 Circuit of an ignition system	3
Figure 1.2 Schematic of the breakdown phase (adapted from [16]).....	4
Figure 1.3 The secondary voltage waveform of a breakdown phase.....	4
Figure 1.4 The secondary voltage and secondary current waveforms of a glow phase.....	5
Figure 1.5 General structure of the thesis	9
Figure 2.1 The spark ignition research platform.....	10
Figure 2.2 Laser alignment for electrodes position adjustment.....	11
Figure 2.3 The single electrode spark plug used in this research	11
Figure 2.4 Testing electrodes with different diameters	12
Figure 2.5 MSD Ignition 5527 coil.....	12
Figure 2.6 Control system overview	13
Figure 2.7 The ignition coil driver circuit of an inductive ignition system	14
Figure 2.8 PicoScope 4425 four-channel automotive oscilloscope [34]	15
Figure 3.1 Electric waveforms of the discharge voltage during the breakdown phase.....	17
Figure 3.2 Breakdown voltages of different spark gaps (0.2 mm HV electrode and 0.2 mm ground electrode).....	18
Figure 3.3 HV and ground electrodes diameters impact on breakdown voltage	19
Figure 3.4 Ground electrode diameter impacts on breakdown voltages.....	20
Figure 3.5 Ground electrode diameter impacts on breakdown voltages with 0.2 mm diameter of HV electrode	21
Figure 4.1 Electric waveforms of secondary voltage during glow phase	22
Figure 4.2 Glow voltage curve waveform	23
Figure 4.3 Electric waveform of secondary current curves	23
Figure 4.4 (a) Calculated secondary current curves using the average value of 100 repeats, (b) The zoomed-in ending of the discharge processes.....	24
Figure 4.5 Ground electrode diameter impacts on glow voltages with 3.5 mm diameter of HV electrode	25

Figure 4.6 Ground electrode diameter impacts on glow voltages with 0.2 mm diameter of HV electrode	26
Figure 4.7 Ground electrode diameter impacts discharge energy with the 3.5 mm diameter of the HV electrode	27
Figure 4.8 Ground electrode diameter impacts on discharge energy with 0.2 mm diameter of HV electrode	27
Figure 4.9 Ground electrode diameter impacts on discharge durations with the 3.5 mm diameter of the HV electrode	28
Figure 4.10 Ground electrode diameter impacts on discharge durations with 0.2 mm diameter of HV electrode	29

LIST OF ABBREVIATIONS/SYMBOLS

Abbreviations

AC	Alternating Current
BEVs	Battery Electric Vehicles
DC	Direct Current
EGR	Exhaust Gas Recirculation
FPGA	Field-programmable Gate Array
GHG	Greenhouse Gas
HV	High Voltage
ICEs	Internal Combustion Engines
ICEVs	Internal Combustion Engine Vehicles
IGBT	Insulated-gate Bipolar Transistor
MIE	Minimum Ignition Energy
MOSFET	Metal–oxide–semiconductor Field-effect Transistor
RT	Real-time
SI	Spark Ignition
TCI	Transistor Coil Ignition
TTL	Transistor-transistor Logic
UV	Ultraviolet

Symbols

a	Gas composition constant	[-]
ϕ	Equivalence ratio	[-]
B	Gas composition constant	[-]
d	Spark gap size	[mm]
T	Gas temperature	[K]
V_b	Breakdown voltage	[V]

CHAPTER 1

INTRODUCTION

1.1 Background

In recent years, the need to improve vehicle fuel economy, and reduce CO₂ emissions, has been gaining significant attention because of climate change and energy sustainability concerns. One of the ways to realize this target is to enhance the engine thermal efficiency by adapting technologies such as high compression ratio, boosted intake pressure, lean burn, and charge dilution, i.e., exhaust gas recirculation (EGR) [1]. While these techniques have proved to be effective in improving engine efficiency, they also induce challenges to the combustion process including ignition difficulties, slow burn rate, partial burn or misfire, and escalated cycle-to-cycle variations [2-3].

For the ignition system in spark ignition engines, one of the greatest challenges is to meet the increased ignition energy requirements of lean mixtures ($\phi < 0.7$) and therein to generate a flame kernel reliably under high in-cylinder pressures associated with intake boosted high-load lean-burn conditions [4-5].

1.2 Ignition System and Spark Discharge Principle

A spark-ignition engine (SI engine) is an internal combustion engine, where the combustion process of the air-fuel mixture is initiated by using an electrical discharge from a spark plug [6]. At present, the transistor coil ignition (TCI) system is the most prevalent system in automotive SI engines owing to its design simplicity, low cost, and robust performance. [7].

A typical TCI ignition system, as shown in Figure 1.1, includes a power supply, a control switch, an ignition coil, spark plugs, and necessary wiring [8]. The ignition coil works on the transformer principle [9], and it consists of a primary coil with a smaller number of windings and a secondary coil with a larger number of windings [10]. The primary circuit is controlled via an insulated-gate bipolar transistor (IGBT) switch by an ignition control signal (spark command) [11]. To prepare for a spark, a charging process is initiated when the primary circuit is closed by the IGBT. The primary current increases until the circuit is opened by the IGBT. This time interval is usually termed as the charging duration. When the transistor switch is turned off, the primary current drops rapidly to 0 A [11]. Correspondingly, a high voltage (in the order of tens of kilovolts) is generated in the secondary coil because of the abrupt current change in the primary circuit [11]. The ratio of the primary voltage to the secondary voltage in this process depends on the ratio of the number of windings in the primary coil to the number of windings in the secondary coil [12]. The high voltage from the secondary coil results in a gas ionization process across the spark gap [12], termed as the breakdown event. After the breakdown event, the energy stored in the magnetic field is gradually released to the spark gap, often in a few milliseconds. The time interval for the whole spark discharge process is termed as the spark discharge duration [13].

In an SI engine, the combustion of the air-fuel mixture is initiated by a spark discharge that creates a flame kernel. The spark discharge process can be generally characterized by two phases: a breakdown phase and an arc/glow phase [10].

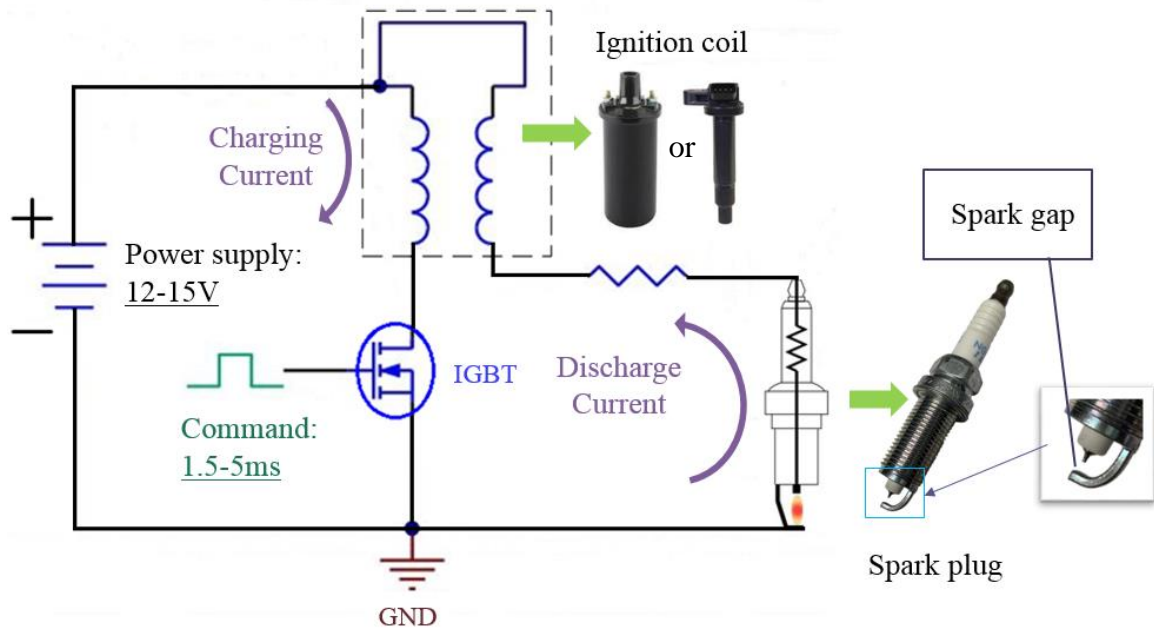


Figure 1.1 Circuit of an ignition system

Breakdown Phase

The spark discharge process begins with a breakdown phase, which occurs at the start of spark discharge. An electric field is developed between the high voltage (HV) electrode and the ground electrode of the spark plug, aided by the energy stored in the ignition coil. The electrons start to move to the anode with the increasing strength of the electrode field. These electrons can also ionize the gas molecules between the spark gap during the collisions, which tends to result in an avalanche effect, i.e., creating a massive increase in the number of electrons and ions. At the same time, the excited atoms also emit low wavelength UV radiation [13-15]. A schematic of the breakdown phase is shown in Figure 1.2.

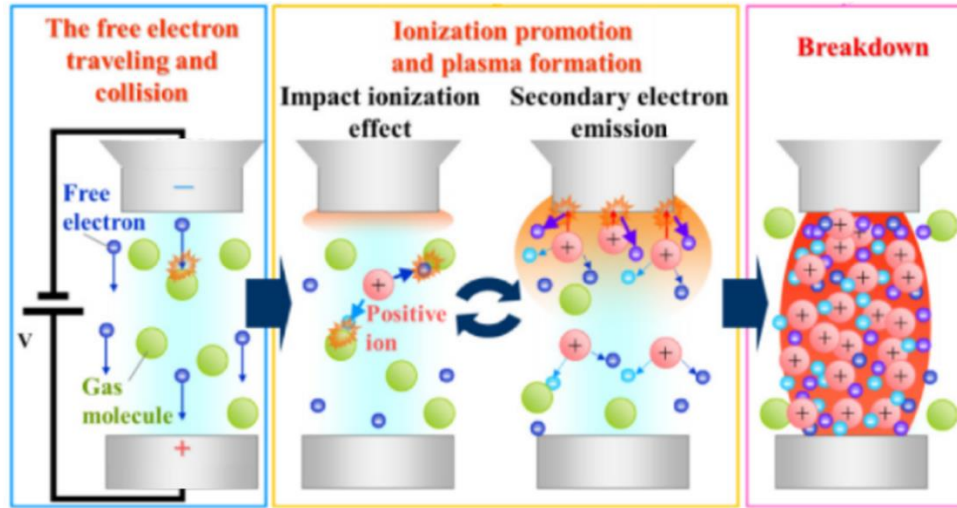


Figure 1.2 Schematic of the breakdown phase (adapted from [16])

The ionized streamers flow between the anode and cathode and create a conductive plasma channel in the spark gap. While the conduction is built up across the HV electrode and the ground electrode of the spark plug, the impedance massively decreases. The energy stored in the parasitic capacitor inside the spark plug, wire, and coil starts to release. The breakdown phase is often characterized by the high voltage as shown in Figure 1.3 (e.g., up to 40 kV), high current (e.g., ~ 200 A), and short duration (e.g., ~ 2 ns) [13-15].

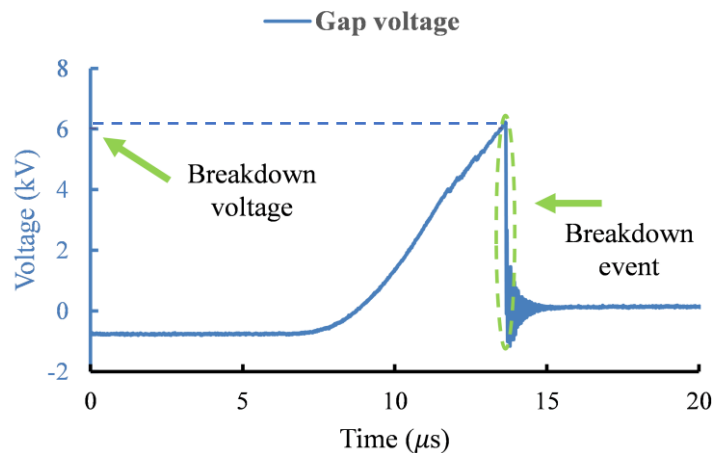


Figure 1.3 The secondary voltage waveform of a breakdown phase

Arc/glow Phase

In the glow phase as shown in Figure 1.4, typically, there is a voltage of 300 to 500 V between the HV and ground electrodes. The glow phase generally lasts for a few milliseconds. In this relatively long discharge process, the ignition circuit releases most of its energy (typically tens of millijoules or higher) [16].

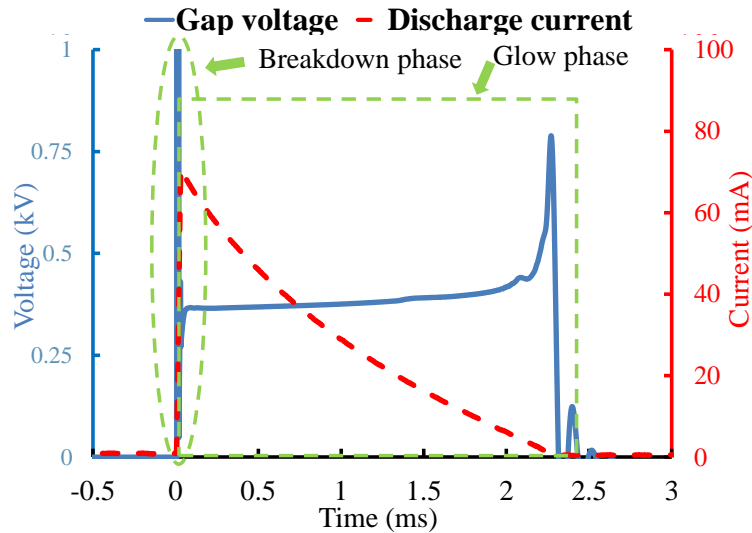


Figure 1.4 The secondary voltage and secondary current waveforms of a glow phase

1.3 Challenges of the Current Ignition Systems

Lean and diluted combustion, along with engine downsizing using turbocharging, are employed to reduce the pumping work of intake throttling, especially at lower engine loads [17]. On the other hand, turbocharged SI engines tend to suffer from greater risk of knocking, and this tendency of knocking may prevent an optimum combustion phasing [17]. EGR, as reported in the literature, has been shown effective in suppressing knock in SI engines [18]. EGR re-uses a percentage of exhaust gas to dilute the engine intake, and it is widely used in diesel engines because of its significant NO_x reduction potential. In

recent years, EGR is being adopted in SI engines to reduce exhaust emission, especially NO_x formation, and to improve the overall thermal efficiency [19].

Although intake charge dilution (either with excessive air or EGR) may help improve engine efficiency and exhaust emissions, dilution often causes challenges for combustion initiation and completion [17]. An excessively lean mixture reduces the propensity for ignition in the vicinity of the spark gap. Charge dilution, especially with EGR, tends to reduce the speed of flame propagation. All of these can lead to a slower burn rate, partial burns or even misfires. Along with stronger air motion that is often implemented to enhance flame propagation in diluted mixtures, significant cycle-to-cycle variations are often observed. Moreover, turbocharging or supercharging (intake boost) causes higher intake charge density, which in turn requires higher breakdown voltage supplied from the ignition system [20-22].

In order to ensure stable ignition and complete combustion under the above conditions, it is important to stabilize the initial flame kernel propagation. Consequently, to-date ignition systems for SI engines should be improved to accommodate these challenging conditions.

1.4 Literature Review

The published research results indicate that different geometrical parameters of spark plug electrodes (both HV electrode and ground electrode), including shape, surface roughness, and material, can affect the discharge characteristics, early flame kernel growth, and overall combustion stability [23-27].

Electrode shape and surface roughness

Liu *et al.* [23] characterized the peak value of electric field strength with the modification of the spark gap. He found that the peak value of electric field strength decreases with the increase of the electrode gap. The arc resistances were higher for the larger electrode gaps, which increased the discharge efficiencies. Spherical electrode had the smallest peak field strength, making it more difficult to achieve the breakdown. The electrode shape had no significant effect on spark resistance and spark energy release efficiency.

A correlation between the electrode surface roughness and the breakdown voltage has been theoretically and experimentally discussed in the literature [24-26]. Sato *et al.* [26] studied a high-voltage electrode made of copper. The following equation describes the relationship between the breakdown voltage and electrode surface roughness:

$$V_{50} = AR^{-n} \quad (1)$$

Where V_{50} is the 50% of the breakdown voltage, R is defined as the centerline average roughness (ISO 468-1982 and ISO 4284/11984), and A and n are the constants formulated as a function of the gap length. This relationship indicates that the increasing electrode surface roughness exponentially decreases the breakdown voltage [25].

Electrode material

Liu *et al.* [23] used copper and tungsten to test the impact of electrode materials on spark discharge: copper and tungsten were found to have no effect on the distribution of the electrostatic field strength across the gap. The differences in the energy losses of tungsten and copper electrodes were insignificant.

Impact of electrode geometry on combustion

Bane *et al.* [27] suggested that the plasma channel emitted a blast wave that was spherical near the electrode surfaces and cylindrical near the center of the spark gaps, and thus, the spark was highly influenced by the electrode geometry. Initially, the flow field following a spark discharge was induced by the blast wave emitted from the high-temperature, high-pressure spark channel. The nature of the blast wave depended on the electrode geometry; and consequently, the details of the fluid mechanics of the evolving spark kernel were greatly influenced by the electrode shape and spacing.

1.5 Objective of the Thesis

It is evident from the published literature that for the spark plugs used in SI engines, different diameters of electrode influence the spark discharge process. The objective of this work is to investigate the effects of electrode diameters on the spark discharge parameters, including the breakdown voltage, secondary voltage during the glow phase (hereafter named “glow voltage”), discharge energy, and discharge duration. The secondary current and voltage were measured. The impacts of the diameters of the HV and ground electrodes on the discharge characteristics have been investigated.

1.6 Structure of the Thesis

The general structure of the thesis is outlined in Figure 1.5.

Preparatory Work	<p>Chapter 1 Introduction</p> <ul style="list-style-type: none"> • Background • Ignition system and its spark discharge principle • Challenges of the current ignition system • Literature review • Objective of the thesis
Methodology	<p>Chapter 2 Experimental setup</p> <ul style="list-style-type: none"> • Overview of the experimental setup • Spark plug • Ignition coil • Control system • Measurement and data collection devices
Analysis Work	<p>Chapter 3 The impact of different electrodes diameters on breakdown voltage</p> <ul style="list-style-type: none"> • Data process and calculation method of breakdown voltages • The impact of different HV and ground electrodes on breakdown voltages
	<p>Chapter 4 The impact of different spark gap sizes and diameter sizes of electrode on breakdown voltage</p> <ul style="list-style-type: none"> • The impact of different HV and ground electrodes on glow voltages, discharge energy, and discharge duration • Discharge result analysis
	<p>Chapter 5 Conclusions and future work</p> <ul style="list-style-type: none"> • Conclusions • Future work

Figure 1.5 General structure of the thesis

CHAPTER 2

EXPERIMENTAL SETUP

2.1 Overview of the Experimental Setup

To investigate the effects of electrode diameters on the spark discharge behavior, an ignition research platform was used. A simplified schematic of the research platform is shown in Figure 2.1. A National Instruments (NI) real-time (RT) controller with an embedded device of field-programmable gate arrays (FPGA) was used to control the ignition system. A host computer with LabVIEW software was used as a user interface linked to the RT-FPGA via an ethernet cable to promptly deliver the command signals. An oscilloscope was used to acquire the trigger, secondary voltage, and secondary current during a spark discharge event for later analysis.

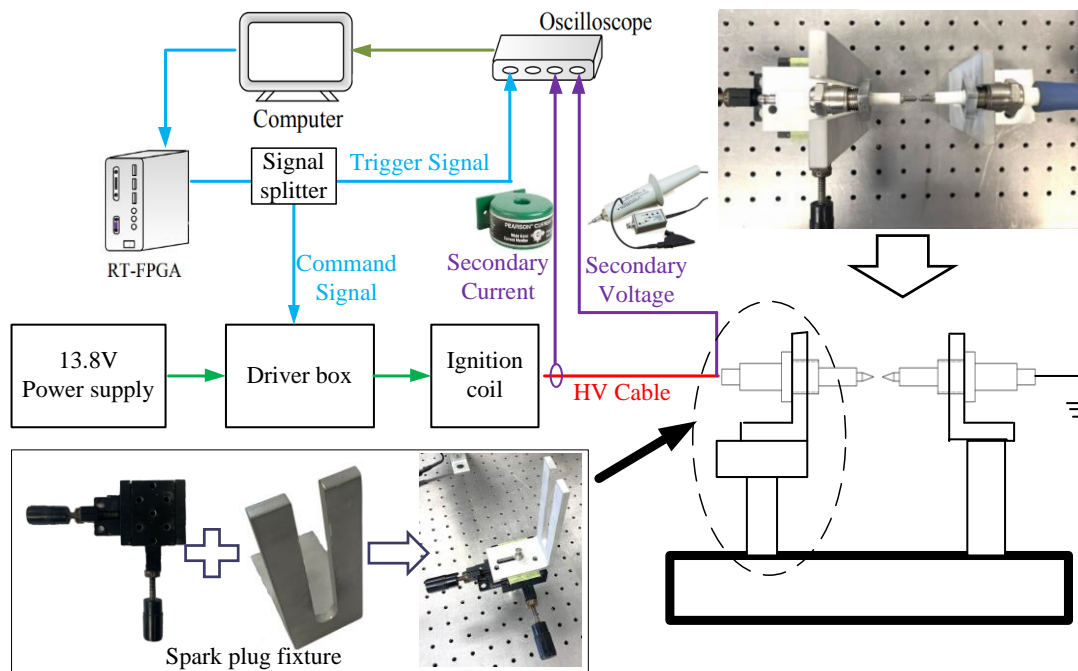


Figure 2.1 The spark ignition research platform

One spark plug was used for spark discharge, and the opposing spark plug was used as the ground. A laser alignment tool was used for spark plug alignment to ensure the electrode surfaces could be parallel to each other, as shown in Figure 2.2.

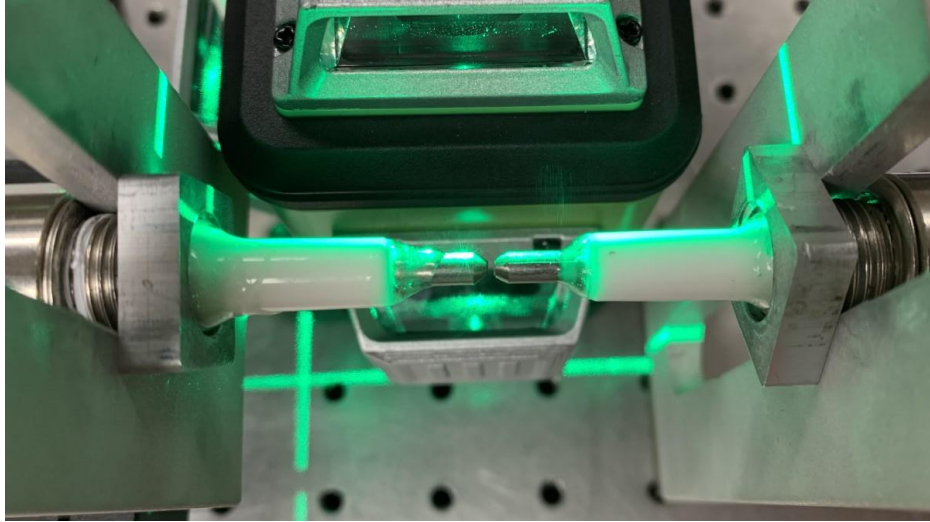


Figure 2.2 Laser alignment for electrodes position adjustment

2.2 Spark Plug

In this research, single electrode spark plugs were used as shown in Figure 2.3. This spark plug had an extended stainless-steel electrode with no ground electrode.



Figure 2.3 The single electrode spark plug used in this research

The spark plug electrodes were shaped to four different diameters, as shown in Figure 2.4. The original diameter of the electrodes was 3.5 mm diameter while the electrode tips were machined to three other diameters, i.e., 0.2 mm, 0.7 mm, and 1.5 mm (Figure 2.4).

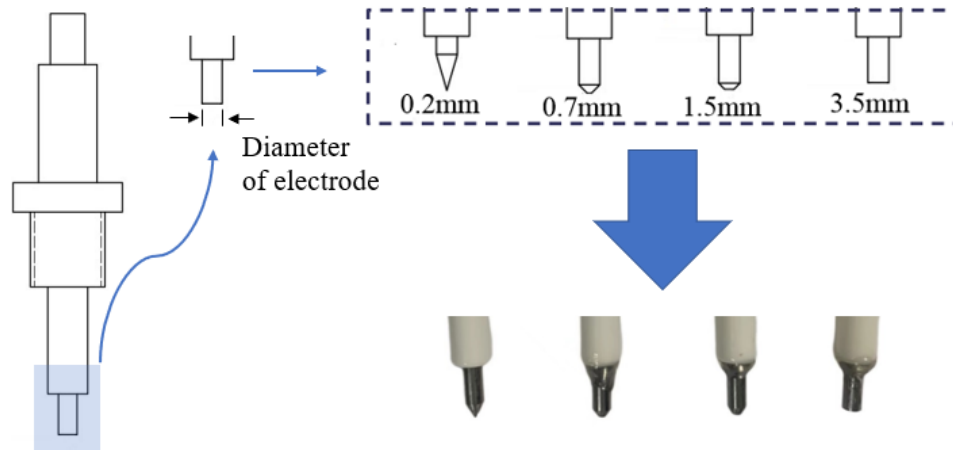


Figure 2.4 Testing electrodes with different diameters

2.3 Ignition Coil

As shown in Figure 2.5 below, an MSD Ignition 5527 coil [28] was used as the ignition coil. The specifications of this coil are summarized in Table 2.1.



Figure 2.5 MSD Ignition 5527 coil

Table 2.1 Specifications of MSD Ignition 5527 coil

Product line	MSD-5527
Primary resistance	0.40 Ω
Turns ratio	100:1
Secondary resistance	3.60 k Ω
Primary inductance	5.20 mH
Maximum voltage	40 kV

2.4 Control System

In this research platform, the ignition command was generated by the NI RT-FPGA system, and the ignition command was split to the ignition coil driver and measurement hardware. The overview of the control system is shown in Figure 2.6.

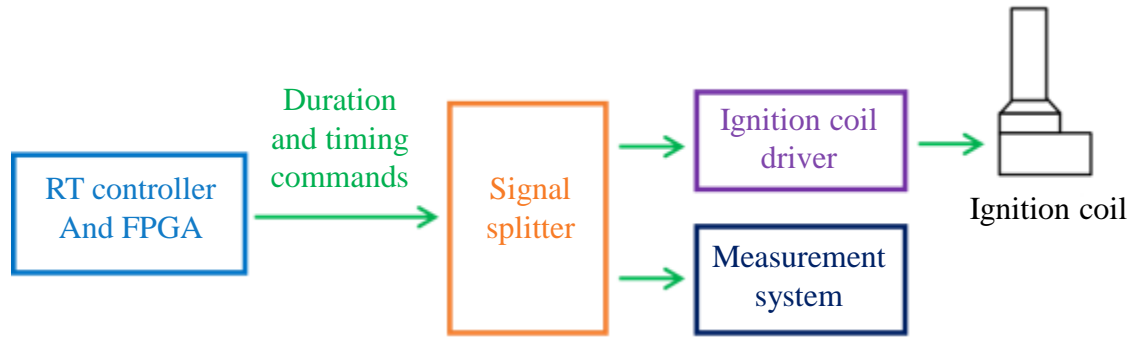


Figure 2.6 Control system overview

2.4.1 Signal Splitter

The command signal was split to be used for the drive command of the ignition coil and the trigger for the data acquisition system. The signal splitter contained a Texas Instruments SN74HC08N AND gate chip [29]. By using this circuit, the signal could be split with negligible voltage loss.

2.4.2 Ignition Coil Driver

An ignition coil driver was used to energize the ignition coil. A schematic of the ignition coil hardware is shown in Figure 2.7. A TTL signal, as the spark command signal, was delivered to a GATE driver (Texas Instruments UCC 37322) [30], which provides high gate drive currents to control the insulated-gate bipolar transistor (IGBT) (ISL9V3040P3) [31].

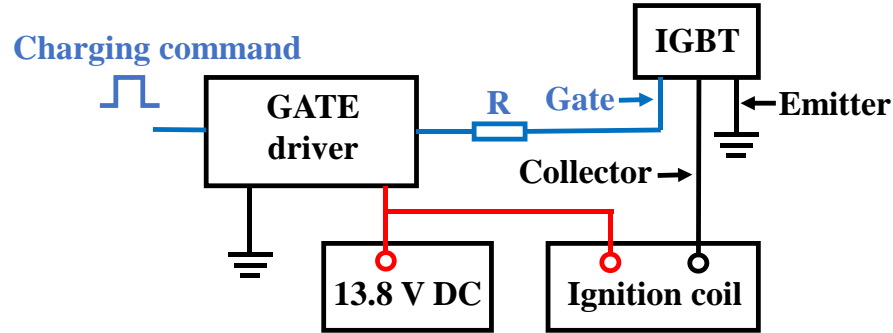




Figure 2.7 The ignition coil driver circuit of an inductive ignition system

2.5 Measurement and Data Acquisition Devices

2.5.1 Measurement Devices

A Tektronix P6015A high voltage probe [32] was used to measure the secondary voltage. The secondary current was measured by a Pearson 411 wideband current monitor [33]. When electric current flows through a conductor, a magnetic field is generated around the conductor. The magnetic field amplitude is proportional to the current flow. The Pearson 411 current monitor measures the strength of the magnetic field and outputs a corresponding electric signal. The specifications of the high voltage probe and the current monitor are shown in Table 2.2.

Table 2.2 Specifications of the data acquisition devices

Picture	Model Number	Measurement Range	Bandwidth
	Tektronix P6015A	20 kV DC / 40 kV Pulsed	DC to 75 MHz
	Pearson TM 411 Wideband	Up to 5000 A	1 Hz to approximately 20 MHz

2.5.2 Data Acquisition Devices

Electric waveforms from the signal splitter, secondary voltage, and secondary current were collected by the oscilloscope [34] as shown in Figure 2.8. An overview of the oscilloscope specifications is summarized in Table 2.3.



Figure 2.8 PicoScope 4425 four-channel automotive oscilloscope [34]

Table 2.3 Specifications of the PicoScope 4425

Model	PicoScope 4425
Channels	4
Bandwidth	20 MHz
Resolution	12 bits
Sampling rate	400 MS/s
Buffer memory	250 M samples
Input range (full scale)	± 50 mV to ± 200 V in 12 ranges

CHAPTER 3

THE IMPACT OF ELECTRODES DIAMETERS ON BREAKDOWN VOLTAGE

In this chapter, the impact of electrode diameter on the breakdown voltage is discussed.

3.1 Data Processing and Calculation Method of the Breakdown Voltage

Even under the same boundary condition, the breakdown voltages show random scattering within a certain range. The breakdown voltage measurements were repeated one hundred times under each test condition. The average value of breakdown voltage was reported for each testing condition.

The electric waveforms of discharge voltage during the breakdown phase are shown in Figure 3.1. The boundary conditions are listed as follows: the spark gap size varies from 0.5 mm to 1.5 mm in 0.2 mm increments, under 1 bar abs. ambient pressure, and a temperature of 25 °C. The gas media was air, and the diameters of the HV electrode and ground electrode were both 0.2 mm. The sampling rate was 20 MHz.

As shown in Figure 3.2, it is observed that the breakdown voltage increases with the increase of spark gap size, which is already proven in previous research extensively and is verified in this study [35]. The error bars indicate the range of the values of the one hundred events and same as all following figures with error bars in this thesis. When the spark gap size is 0.5 mm, the breakdown voltage is 8.07 kV, and with the spark gap size of 1.5 mm, the breakdown voltage is increased to 10.59 kV.

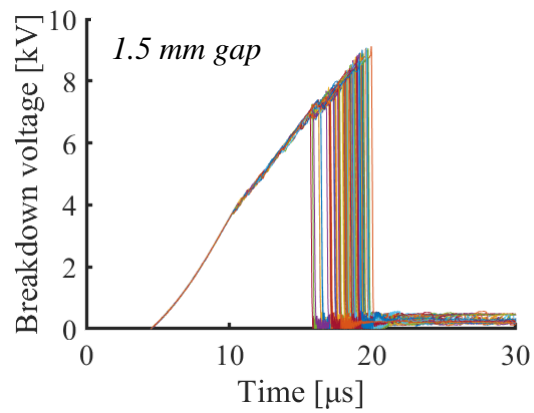
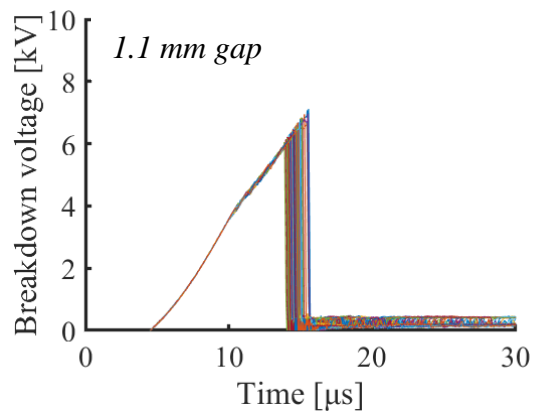
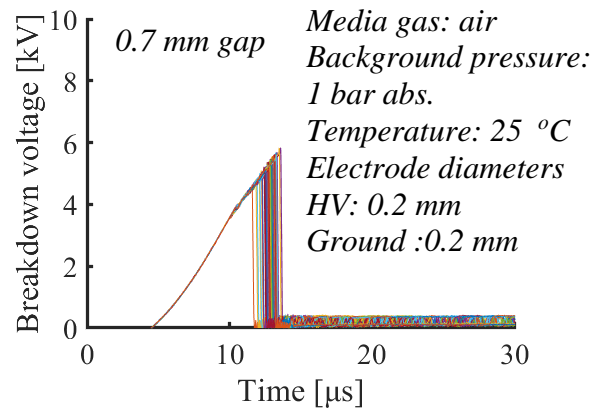


Figure 3.1 Electric waveforms of the discharge voltage during the breakdown phase

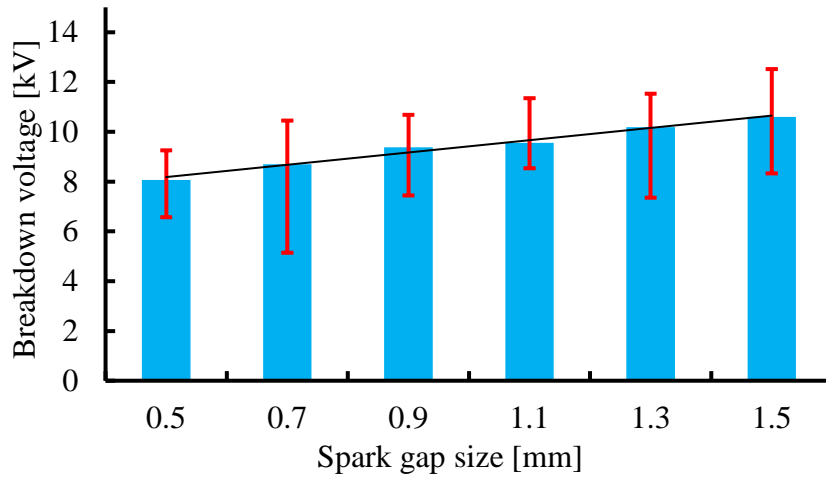


Figure 3.2 Breakdown voltages of different spark gaps (0.2 mm HV electrode and 0.2 mm ground electrode)

3.2 Impact of Electrodes Diameter on the Breakdown Voltage

The impact of electrode diameter on breakdown voltage is shown in Figure 3.3. At 1.5 mm spark gap size, the setup with 3.5 mm diameter of both the HV and ground electrodes needed 16.58 kV to breakdown. Meanwhile, once the 0.2 mm diameter electrode was used as either the HV or the ground electrode, the breakdown voltages were much lower. However, when the spark gap size was small (0.5 mm and 0.7 mm), the impact of electrode diameters on breakdown voltage was less significant.

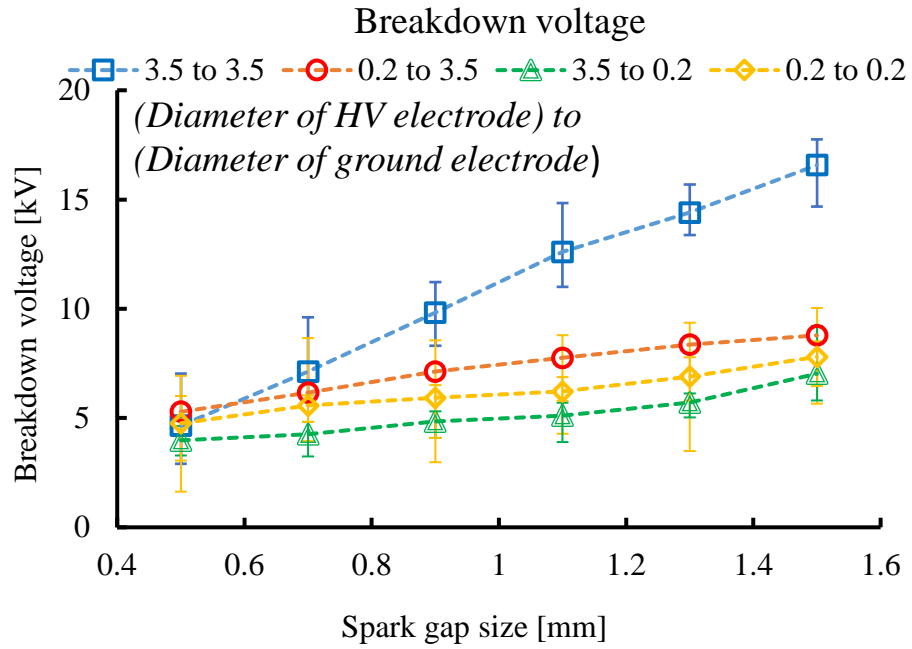


Figure 3.3 HV and ground electrodes diameters impact on breakdown voltage

To further investigate the effect of electrode diameters on breakdown voltage, more tests were performed with two other ground electrode diameters of 0.7 mm and 1.5 mm. Results were shown in Figure 3.4. The uses of 0.7 mm and 1.5 mm diameters of ground electrodes produced similar breakdown voltages under various spark gap sizes. The 0.2 mm diameter of the ground electrode produced the lowest breakdown voltages under all spark gap sizes.

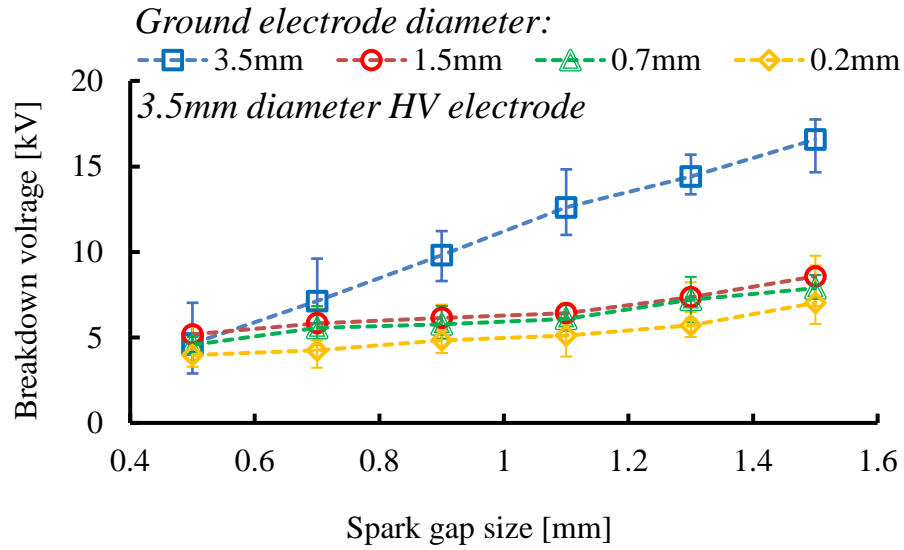


Figure 3.4 Ground electrode diameter impacts on breakdown voltages

Further tests were conducted using the 0.2 mm diameter electrode as the HV electrode, as shown in Figure 3.5. The breakdown voltages when the diameter of ground electrode changes from 0.7 to 3.5 mm were remarkably close. While the 0.2 mm HV and 0.2 mm ground electrode setup resulted in the lowest breakdown voltages, on average 10% to 15% lower compared with other conditions. The point discharge theory can be considered to explain the phenomenon: under the action of a strong electric field, where the surface of the object has a large curvature (such as the top of a sharp and small object), it is easier to cause the gas near the surface to be ionized to generate discharge [15].

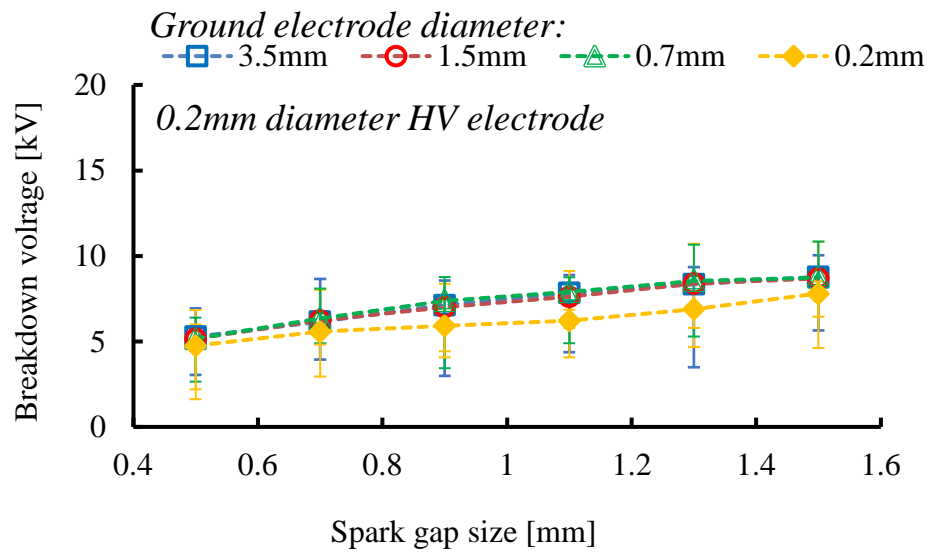


Figure 3.5 Ground electrode diameter impacts on breakdown voltages with 0.2 mm diameter of HV electrode

CHAPTER 4

THE IMPACT OF ELECTRODE DIAMETER ON GLOW PHASE

In this chapter, empirical results are reported and discussed on the impact of various sizes of HV and ground electrodes diameters on discharge energy, discharge duration, and the glow voltage. The sampling rate was set to 1 MHz.

Figure 4.1 shows the secondary voltage curves of 100 repeated spark events under the same condition (0.7 mm spark gap size, 0.2 mm diameter of HV electrode, and 0.2 mm diameter of ground electrode). Unlike the breakdown voltage, the secondary voltages exhibited much better consistency.

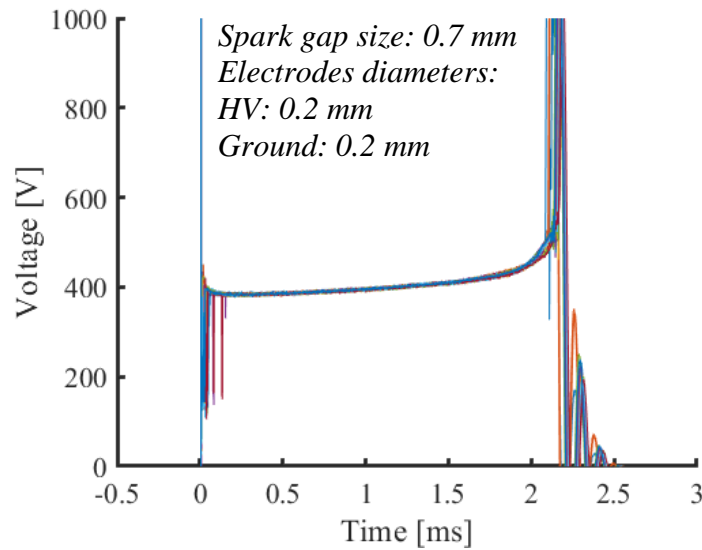


Figure 4.1 Electric waveforms of secondary voltage during glow phase

Figure 4.2 shows the curve of averaged glow voltage using the average value of 100 repeated spark events. In this work, the glow voltage value is subtracted from the average glow voltage from 0.5 ms to 1 ms after the spark command (shown in the blue highlighted zone in Figure 4.2).

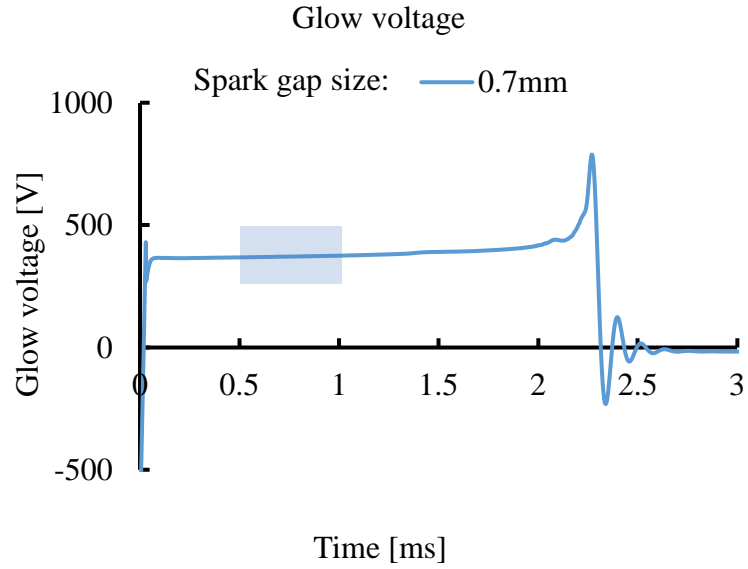


Figure 4.2 Glow voltage curve waveform

The secondary current data was shown in Figure 4.3.

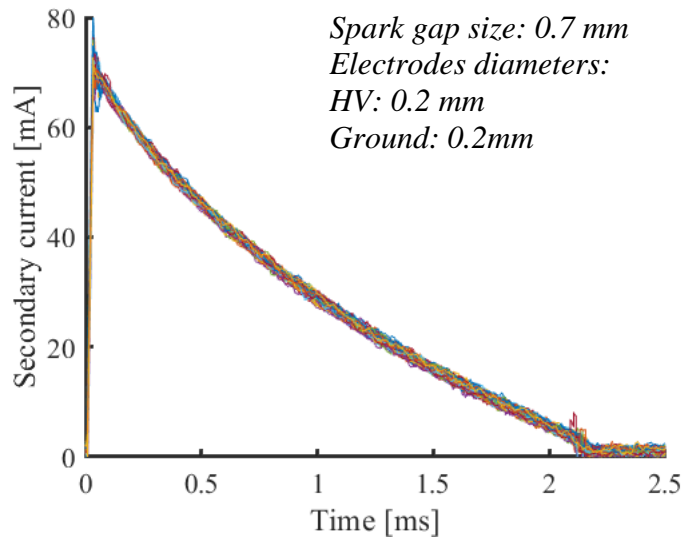
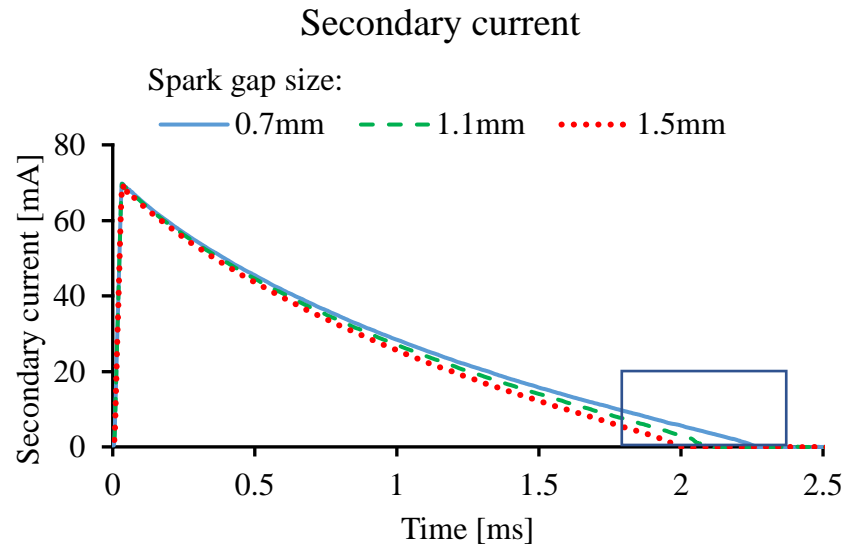
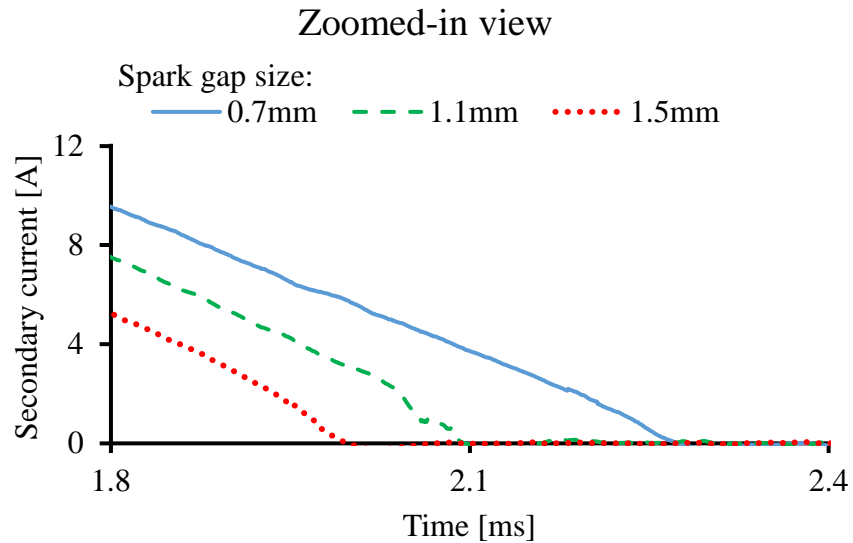


Figure 4.3 Electric waveform of secondary current curves

Figure 4.4 (a) shows the curve of calculated secondary current using the average value of 100 repeats, for various spark gap sizes.



(a)



(b)

Figure 4.4 (a) Calculated secondary current curves using the average value of 100 repeats, (b) The zoomed-in ending of the discharge processes

Figure 4.4 (b) shows the end of the spark discharge process. The time interval between the start of the discharge and the end of discharge is termed as the spark discharge duration.

4.1 Impact of Electrodes Diameter on the Glow Voltage

Figure 4.5 shows impact of ground electrode diameter on glow voltage. The 3.5 mm diameter HV and 3.5 mm ground electrodes showed in the lowest glow voltage, and the smallest (0.2 mm) diameter of the ground electrode for this test showed the highest glow voltages under all spark gap sizes. It is indicated that smaller diameter electrodes resulted in higher glow voltages.

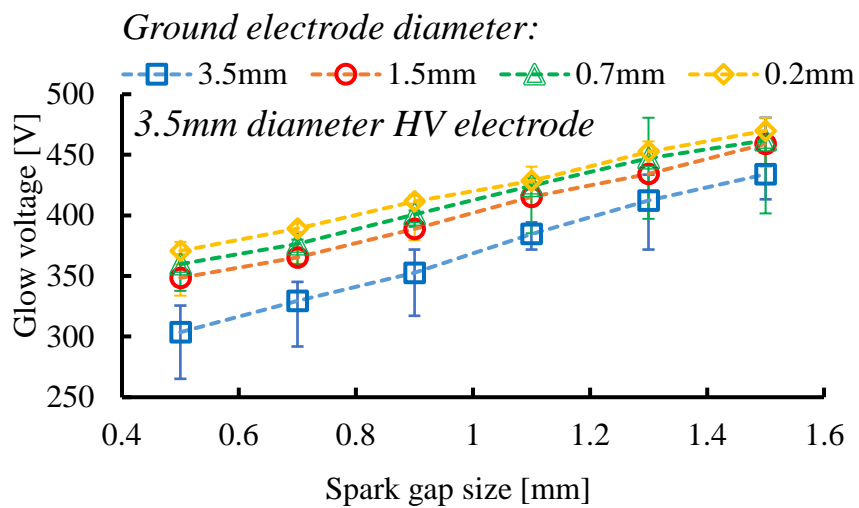


Figure 4.5 Ground electrode diameter impacts on glow voltages with 3.5 mm diameter of HV electrode

The tests were repeated using the 0.2 mm diameter HV electrode and the results were shown in Figure 4.6. The glow voltage was not sensitive to ground electrode diameters when HV electrode diameter was 0.2 mm.

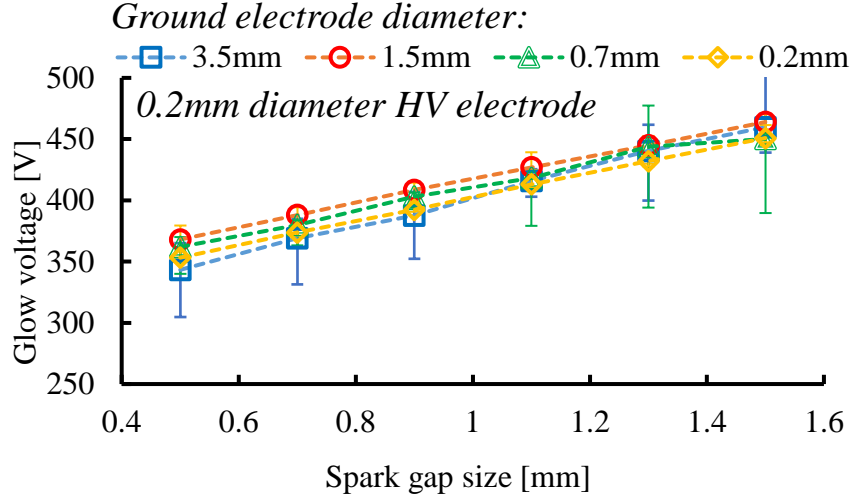


Figure 4.6 Ground electrode diameter impacts on glow voltages with 0.2 mm diameter of HV electrode

4.2 Impact of Electrodes Diameter on the Discharge Energy

The discharge energy, i.e., the electric energy delivered to the spark gap, was calculated by integrating the product of secondary voltage and current over the discharge duration, as expressed in the equation below.

$$E_{discharge} = \int_0^t U_{glow}(t) I_{secondary}(t) dt \quad (2)$$

Where E is the discharge energy, U_{glow} is the secondary voltage, I is the secondary current, and t is the time.

Figure 4.7 shows the impact of electrode diameter on discharge energy. All setups except using the 3.5 mm for both HV and ground electrode diameters, exhibited very similar discharge energies for all spark gaps. The test with 3.5 mm HV and ground electrodes on different spark gap sizes showed an average of 7 mJ lower discharge energy than those of smaller ground electrodes.

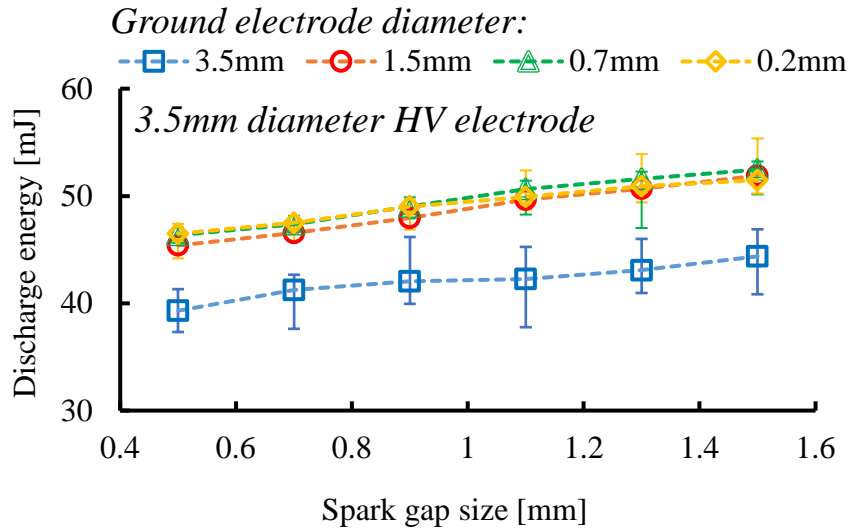


Figure 4.7 Ground electrode diameter impacts discharge energy with the 3.5 mm diameter of the HV electrode

Compared with the discharge energy when using a 3.5 mm diameter HV electrode, using the 0.2 mm diameter HV electrode exhibited similar results over various ground electrode diameters, as shown in Figure 4.8. Nonetheless, while using the 3.5 mm diameter ground electrode, the discharge energy is <5% lower than those of smaller ground electrodes, for all spark gaps.

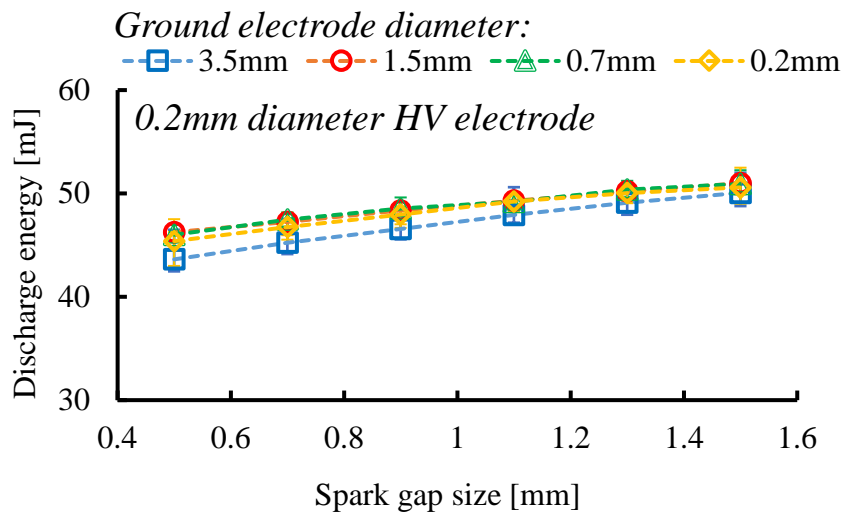


Figure 4.8 Ground electrode diameter impacts on discharge energy with 0.2 mm diameter of HV electrode

4.3 Impact of Electrodes Diameter on the Discharge Duration

Figure 4.9 shows the impact of electrode diameter on the discharge duration. The diameter of the HV electrode was 3.5 mm. Compared with other setups, the 3.5 mm diameter ground electrodes provided the longest discharge duration; and the difference increased under smaller spark gap sizes. The diameter of ground electrode showed minimum impacts on discharge duration when the spark gap was above 1.3 mm.

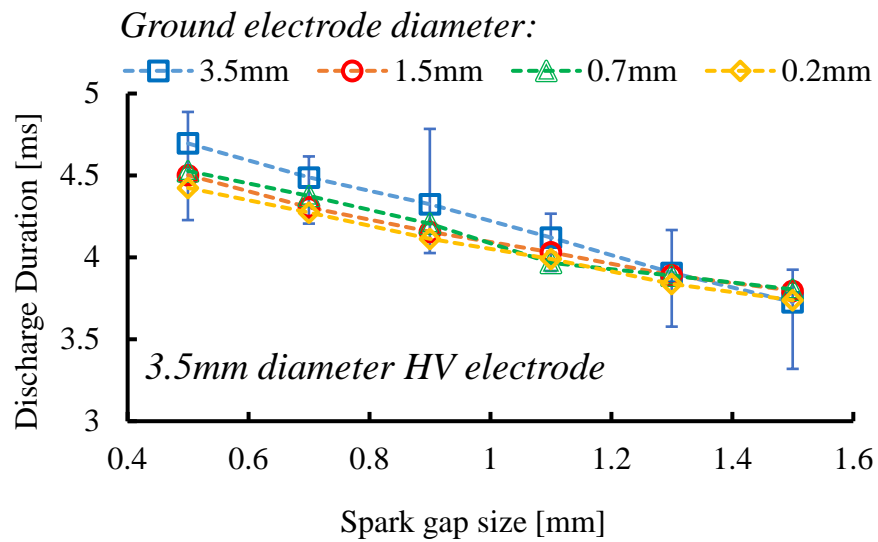


Figure 4.9 Ground electrode diameter impacts on discharge durations with the 3.5 mm diameter of the HV electrode

As shown in Figure 4.10, a 0.2 mm diameter HV electrode showed a larger scatter with the ground electrode diameter. Further, when the diameter of the HV electrode was fixed at 0.2 mm, the larger diameters of the ground electrodes resulted in shorter discharge durations.

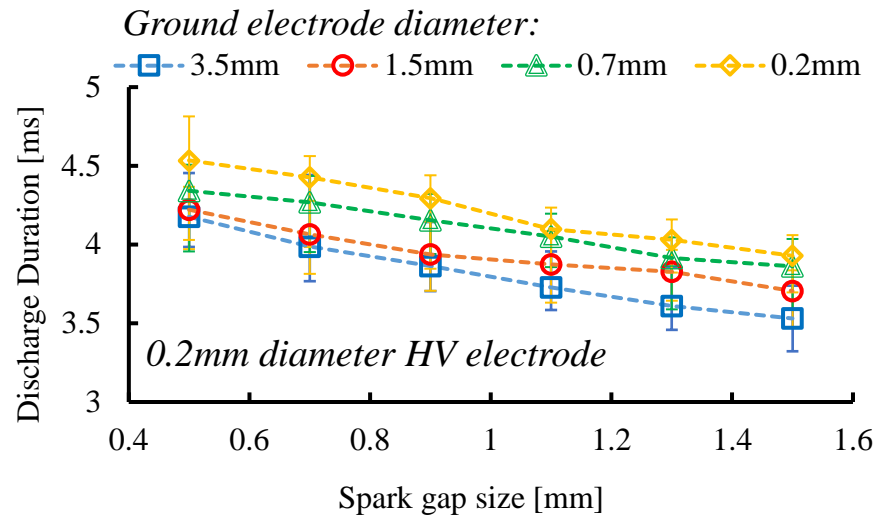


Figure 4.10 Ground electrode diameter impacts on discharge durations with 0.2 mm diameter of HV electrode

CHAPTER 5

CONCLUSIONS AND FUTURE WORK

This work focused on the impact of the electrode diameters (0.2 mm, 0.7 mm, 1.5 mm, and 3.5 mm) on the spark discharge processes. This chapter provides a summary of the research results and conclusions from the work performed.

Recommendations for future research are also provided.

5.1 Conclusions

The impacts of electrode diameter on the spark discharge characteristics were analyzed, and the conclusions are summarized below.

- Under the present testing conditions, the increased diameter of electrodes (including HV and ground) resulted in higher breakdown voltages.
- When the diameter of the HV electrode was 3.5 mm, a larger diameter of the ground electrode resulted in a lower glow voltage. On the other hand, when the diameter of the HV electrode was 0.2 mm, the size of the ground electrode does not show an obvious impact on the glow voltage.
- When the diameter of the HV electrode was fixed at 3.5 mm, an increase in ground electrode diameter resulted in lower discharge energy. When the HV electrode diameter was 0.2 mm, the diameter of the ground electrode did not show an obvious impact on the discharge energy.
- When the diameter of the HV electrode was fixed at 3.5 mm, the size of the ground electrode did not show an obvious impact on the discharge duration.

When the diameter of the HV electrode was fixed at 0.2 mm, the bigger diameter of the ground electrode resulted in a shorter discharge duration.

5.2 Future Work

The experiment was performed under atmospheric conditions. More tests can be carried out under pressurized conditions, which can be related to engine operating conditions.

REFERENCES

1. Hayashi, N., Sugiura, A., Abe, Y., & Suzuki, K. (2017). Development of Ignition Technology for Dilute Combustion Engines. *SAE International Journal of Engines*, 10(3), 984–994. <https://doi.org/10.4271/2017-01-0676>
2. Alger, T., Gingrich, J., Mangold, B., & Roberts, C. (2011). A Continuous Discharge Ignition System for EGR Limit Extension in SI Engines. *SAE International Journal of Engines*, 4(1), 677–692. <https://doi.org/10.4271/2011-01-0661>
3. Galloni, E., Fontana, G., & Palmaccio, R. (2012). Numerical analyses of EGR techniques in a turbocharged spark-ignition engine. *Applied Thermal Engineering*, 39, 95–104. <https://doi.org/10.1016/.2012.01.040>
4. Yu, S., & Zheng, M. (2021). Future gasoline engine ignition: A review on advanced concepts. *International Journal of Engine Research*, 22(6), 1743–1775. <https://doi.org/10.1177/1468087420953085>
5. Dale, J., Checkel, M., & Smy, P. (1997). Application of high energy ignition systems to engines. *Progress in Energy and Combustion Science*, 23(5), 379–398. [https://doi.org/10.1016/S0360-1285\(97\)00011-7](https://doi.org/10.1016/S0360-1285(97)00011-7)
6. Basshuysen, R., Schaefer, F., & TechTrans. (2016). *Internal Combustion Engine Handbook* (2nd ed.). Warrendale: SAE International. <https://doi.org/10.4271/R-434>

7. Zhu, H. (2018). *Spark Energy and Transfer Efficiency Analyses on Various Transistor Coil Ignition Systems* (Master's thesis). ProQuest Dissertations & Theses Global. (2048175833)
8. Paul C. Kline. (1970). Some Factors to Consider in the Design and Application of Automotive Ignition Systems. *SAE Transactions*, 79, 271–286.
9. Wang, L., Chen, G., Tjong, J., & Zheng, M. (2022). Electrical and Optical Characterization Methodologies for Advanced Spark Ignition. *Journal of Energy Resources Technology*, 144(9). <https://doi.org/10.1115/1.4053437>
10. Bauer, H. (2004). *Gasoline-engine management* (2nd ed., completely rev. and extended.). Plochingen: Robert Bosch.
11. Yang, Z. (2021). *Advanced Ignition Strategies for Future Internal Combustion Engines with Lean and Diluted Fuel-Air Mixtures* (Doctoral dissertation). ProQuest Dissertations & Theses Global. (2493518141).
12. Van Basshuysen, R., & Schäfer, F. (2004). *Internal combustion engine handbook: basics, components, systems, and perspectives*. Warrendale, Pa: SAE International.
13. Wang, L., Chen, G., Tjong, J., & Zheng, M. (2022). Electrical and Optical Characterization Methodologies for Advanced Spark Ignition. *Journal of Energy Resources Technology*, 144(9). <https://doi.org/10.1115/1.4053437>
14. Zhu, H., Yu, X., Yang, Z., Liang, L., & Zheng, M. (2019). Investigation of the Electrical-to-Thermal Energy Transfer Efficiency of Different Discharge Strategies

- Through Electrical and Calorimetry Measurement. *ASME 2019 Internal Combustion Engine Division Fall Technical Conference*. American Society of Mechanical Engineers. <https://doi.org/10.1115/ICEF2019-7232>
15. Abe, Y., Sugiura, A., Shibata, M., Yokoo, N., & Nakata, K. (2015, April). Study of ignition system for demand voltage reduction. In *SAE 2015 World Congress & Exhibition SAE International* (No. 2015-01-0777).
16. Stone, R. (1999). *Introduction to internal combustion engines*. (3rd ed.). Warrendale, PA: Society of Automotive Engineers.
17. Tornatore, C., & Marchitto, L. (2021). Advanced Technologies for the Optimization of Internal Combustion Engines. *Applied Sciences*, 11(22), 142–151. <https://doi.org/10.3390/app112210842>
18. Szybist, J. P., Wagon, S. W., Splitter, D., Pitz, W. J., & Mehl, M. (2017). The Reduced Effectiveness of EGR to Mitigate Knock at High Loads in Boosted SI Engines. *SAE International Journal of Engines*, 10(5), 2305–2318. <https://doi.org/10.4271/2017-24-0061>
19. Alger, T., Gingrich, J., Mangold, B., & Roberts, C. (2011). A Continuous Discharge Ignition System for EGR Limit Extension in SI Engines. *SAE International Journal of Engines*, 4(1), 677–692.
20. Tornatore, C., & Marchitto, L. (2021). Advanced Technologies for the Optimization of Internal Combustion Engines. *Applied Sciences*, 11(22), 10842–10845. <https://doi.org/10.3390/app112210842>

21. Gettel, L. E., & Tsai, K. C. (1983). Flame kernel development with the multiple electrode spark plug. *Combustion and Flame*, 54(1), 225–228. [https://doi.org/10.1016/0010-2180\(83\)90035-4](https://doi.org/10.1016/0010-2180(83)90035-4)
22. Dale, J. D., Checkel, M. D., & Smy, P. R. (1997). Application of high energy ignition systems to engines. *Progress in Energy and Combustion Science*, 23(5), 379–398. [https://doi.org/10.1016/S0360-1285\(97\)00011-7](https://doi.org/10.1016/S0360-1285(97)00011-7)
23. Liu, J., Bi, M., Jiang, H., & Gao, W. (2020). Evaluation of spark discharge. *Journal of Electrostatics*, 107, 103–112. <https://doi.org/10.1016/j.elstat.2020.103500>
24. Morovatiyan, M., Shahsavan, M., Shen, M., & Mack, J. H. (2018). Investigation of the effect of electrode surface roughness on spark ignition. *Internal Combustion Engine Division Fall Technical Conference* (Vol. 51982, p. V001T03A022).
25. Berger, S. (1976). Onset or breakdown voltage reduction by electrode surface roughness in air and SF₆. *IEEE Transactions on Power Apparatus and Systems*, 95(4), 1073–1079. <https://doi.org/10.1109/T-PAS.1976.32199>
26. Sato, S., & Koyama, K. (2003). Relationship between electrode surface roughness and impulse breakdown voltage in vacuum gap of Cu and Cu-Cr electrodes. *IEEE Transactions on Dielectrics and Electrical Insulation*, 10(4), 576–582. <https://doi.org/10.1109/TDEI.2003.1219640>
27. Bane, S. P. M., Ziegler, J. L., & Shepherd, J. E. (2015). Investigation of the effect of electrode geometry on spark ignition. *Combustion and Flame*, 162(2), 462–469. <https://doi.org/10.1016/j.combustflame.2014.07.017>

28. MSD Ignition “Street Fire Blaster TFI Coil PN 5527,” [Online] Available: https://static.summitracing.com/global/images/instructions/msd-5527_frm28609.pdf
[Accessed: 7-September-2022]
29. Texas Instruments “SN74HC08N AND gate chip,” [Online] Available: https://www.ti.com/lit/ds/symlink/sn74hc08.pdf?ts=1660720762106&ref_url=https%253A%252F%252Fwww.ti.com%252Fsite%252Fen-us%252Fdocs%252Funiversalsearch.tsp%253FlangPref%253Den-US%2526searchTerm%253Dsn74hc08n%2526nr%253D9[Accessed: 6-June-2022].
30. Texas Instruments “UCC3732x” [Online] Available: https://www.ti.com/lit/ds/symlink/ucc27321.pdf?ts=1660807129899&ref_url=https%253A%252F%252Fwww.google.com%252F[Accessed: 6-June-2022].
31. Fairchild Semiconductor, “ISL9V3040P3 n-channel ignition IGBT,” [Online] Available: <https://www.onsemi.com/pdf/datasheet/isl9v3040d-f085-d.pdf> [Accessed: 6-June-2022].
32. Tektronix, “P6015A high-voltage probe,” [Online] Available: <https://www.tek.com/datasheet/passive-high-voltage-probes> [Accessed: 6-June-2022].
33. Pearson Electronics., “Pearson current monitor model 411,” [Online] Available: <http://pearsonelectronics.com> [Accessed: 6-June-2022].
34. Pico Technology, “PicoScope 4425 data sheet,” [Online] Available: <https://www.picotech.com/download/manuals/picoscope-4425-data-sheet.pdf> [Accessed: 6-June-2022].

35. Belmouss, M. (2015). *Effect of electrode geometry on high energy spark discharges in air* (Master's thesis). ProQuest Dissertations Publishing. (1716338347)

VITA AUCTORIS

NAME:	Hongyang Shangguan
PLACE OF BIRTH:	Jining, Shandong, China
YEAR OF BIRTH:	1991
EDUCATION:	The University of Texas at Dallas, B.Sc., Texas, U.S. 2018